THE JOURNAL OF PHYSICAL CHEMISTRY B

Article

pubs.acs.org/JPCB

Influence of Spacer–Receptor Interactions on the Stability of Bivalent Ligand–Receptor Complexes

Jorge Numata,[†] Alok Juneja,[†,‡] Dennis J. Diestler,[†,§] and Ernst-Walter Knapp*[,†]

[†]Department of Biology, Chemistry and Pharmacy, Institute of Chemistry and Biochemistry, Fabeckstrasse 36A, D-14195 Berlin, Germany

[‡]Department of Biosciences and Nutrition, Karolinska Institutet, SE-141 83 Huddinge, Sweden

[§]University of Nebraska-Lincoln, Lincoln, Nebraska 68583, United States

Supporting Information

ABSTRACT: Experiments show that a ligand–receptor complex formed by binding a bivalent ligand (D) in which the two ligating units are joined covalently by a flexible polymeric spacer (S) can be orders of magnitude more stable than the corresponding complex formed with monomeric ligands. Although molecular models rationalizing this "enhancement effect" have been proffered, they ignore spacer–receptor (S–R) interactions, which can substantially influence the relative stability of complexes. Here, the results of a computational study designed to assess the impact of S–R interactions in the prototypic bivalent complex are presented and compared to results of experiments. The S–R interactions mimicking general features of biological systems are modeled by contoured R surfaces with hills (or depressions) at the binding sites. In the fictitious limit of vanishing S–R interactions, the enhancement is pronounced, as observed in experiments. For strictly repulsive S–R interactions (hard R surface), the enhancement vanishes, or even reverses. This is particularly the case if the R surface is convex (i.e., rising between the binding sites), while the enhancement is only moderately reduced if the R surface is concave. Alternatively, a weak S–R attraction close to the R surface can increase the enhancement. It is concluded that large enhancement should be observed only if both features are present: a concave R surface plus a weak S–R attraction. The latter occurs for spacer material such as polyethylene glycol (PEG), which is weakly hydrophobic and thus attracted by protein surfaces. It is shown that the enhancement of bivalent binding can be characterized by a single key parameter, which may also provide guidelines for the design of multivalent complexes with large enhancement effect.

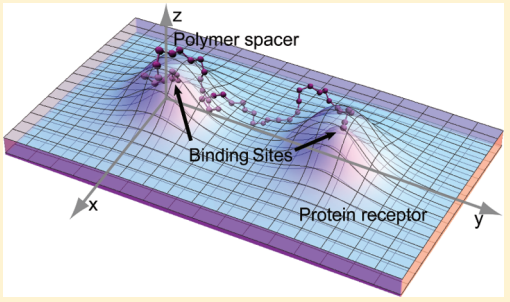

1. INTRODUCTION

Multivalent ligand–receptor complexes consist of associations of molecules held together by multiple, simultaneous, noncovalent bonds. They play essential roles in many natural (biological) processes,[1−4] in medicinal chemistry for the design of new therapeutics,[5,6] as well as in the synthesis of artificial supramolecular systems.[7−11] To delineate the nature of multivalent complexes, we focus on a prototypal molecular system, the bivalent complex in which a bivalent (or divalent) ligand (D) binds to a bivalent receptor (R). We assume that D is constructed by covalently joining two monovalent ligands (M's) via a spacer (S) (e.g., a polymer chain). Note that we replace the term "linker" used in earlier works[12,13] by "spacer" (denoted "S") to emphasize that S imposes a constraint on the distance between the monomeric ligating units. The resulting D then consists of two ligating units connected by S. The bivalent complex forms as the units ensconce themselves in the two binding sites of R, which one can visualize as "pockets" formed by groups of atoms in special configurations so as to conform to the ligating units (i.e., the unit and the binding site are physicochemically complementary; they accommodate each other through specific, unique interactions). We further assume that the ligating units, which in essence are M's modified by virtue of a covalent bond to S, practically do not differ from the original (free) M's in their chemical nature.

By a judicious choice of S, one can construct a multivalent complex whose thermodynamic stability is far greater than that of its monovalent counterpart.[14−29] To be specific, we note that the stability of the prototype, in which both ligating units of D bind to the two binding sites of R, can be enhanced relative to that of the monovalent complex, in which two M's independently bind to the two sites of R. This "enhancement effect" has an important practical implication, which is that a desired effect initiated by formation of a bivalent complex can be accomplished at concentrations of D much lower than those required of the monovalent counterpart.

It should be noted that the term enhancement effect, which implies that the stability of the bivalent complex increases relative to that of the monovalent counterpart, reflects the prejudice that one should achieve a desired effect using as little of the presumably precious (or toxic, if it involves undesirable side effects) M as possible. In principle, if D is designed poorly,

Received: November 26, 2011
Revised: January 22, 2012
Published: January 26, 2012

the stability of the bivalent complex may just as well be less than that of its monovalent counterpart.

In previous articles,[12,13] we developed a fundamental theory of the enhancement effect and compared its predictions with the results of experimental studies of the binding of cyclic guanidine monophosphate (cGMP) ligands, which activate nucleotide-gated ion channels in bovine rod photoreceptor cells (RET).[14] Applying classical statistical mechanics to the prototypal molecular system, we derived closed expressions for the binding constants in terms of molecular properties. Among the approximations that were introduced to permit derivation of analytic formulas was the complete neglect of all spacer−receptor (S−R) interactions as is generally done in theoretical descriptions of multivalent binding. Despite these simplifications, the agreement between theory and experiment is reasonably good.

Recently, a very simple model for S−R interactions (purely repulsive, planar R) was used in a Monte Carlo study of multivalent binding of functionalized nanoparticles.[30] The purpose of this Article is to present the results of a systematic study of a realistic topographical model designed to assess the influence of S−R interactions on the enhancement effect. The topography of the R surface is varied between convex and concave, and weak S−R attractions are considered. Such weak attraction has been shown to exist between protein surfaces and polyethylene glycol (PEG),[31−37] often used as spacer material. We find that S−R interactions can play a significant role in altering the relative stability of complexes, which can also have a strong impact on the ligand's biological activity. In light of our present study, the reasonable agreement between experiment and our model[12,13] that ignores S−R interactions must be regarded as fortuitous, resulting from cancellations of errors. In the present study, we attempt to clarify why a generally expected enhancement of bivalent ligand binding relative to the monovalent case often fails to appear for unfavorable choices of R and S.

2. THEORY

2.1. Description of Prototypal Model. We adopt the "local" nomenclature employed in earlier work.[12,13] We take the binding sites of R to be equivalent and the ligating units of D to be equivalent. The symbol $RD^{(1)}$ stands for the complex in which a single unit of one D is bound to a site of R, $RD^{(2)}$ for the R complex in which the two units of the same D bind to both sites of R, and $RD^{(1)}{}_2$ for the complex in which units of two different Ds bind to the two sites of R.

We treat R as an extended rigid body and M (or the ligating unit) as an atom-like point mass, neglecting internal degrees of freedom of both. We envisage the two binding sites of R to be pockets formed by atoms in fixed configurations. The M's (or ligating units) are planted in the sites to form the complex. D is constructed by covalently connecting two M's via a generally flexible S-chain (henceforth, S is taken to be a polymer chain). We assume that the physicochemical character of the ligating units in D is practically the same as that of the M's alone. Except for the binding interaction, additional (nonspecific) interactions of the ligating units themselves with R are ignored. This approximation is justified, because the ligating units of D and the corresponding M's are subject to the same nonspecific interactions with R. The S−R interaction $U^{(SR)}$ is based on an R model with an atomically smooth, hard surface, impenetrable to atoms of S, with an attractive layer above it. The R surface has hills or depressions at the sites, so that the topography between the sites can be characterized as concave (for hills) or convex (for depressions).

2.2. Canonical Molecular Partition Functions (q) and Binding Constants (K). We restrict our consideration to solutions sufficiently dilute that intermolecular interactions between different D's or different R's can be neglected. Interpreting $U^{(SR)}$ as potential of mean force, we implicitly account for the influence of solvent. Under these conditions, the binding constants of the complexes can be expressed simply in terms of canonical partition functions (q) of the isolated species. In prior work,[13] we derived formulas for these q's under assumptions that differ from the present study in several respects. Here, we focus on the prototypic bivalent rather than a tetravalent R and take M (and the ligating unit) to be atom-like rather than an extended rigid body, as we continue to treat R. Although these approximations may appear to be severe, they do not affect the essential conclusions of the study. Previously, we formally accounted for symmetries of the different molecular species,[13] but ignored them in comparing the predictions of the model with results of the experiment.[14] Here, the molecular symmetries are considered explicitly. Finally, and most important, the S−R interactions $U^{(SR)}$, which were neglected in former treatments, are included in the present one. Indeed, our focus is on the effects of $U^{(SR)}$ on the stability of the bivalent complex relative to its monovalent counterpart.

In appendix A of the Supporting Information, we derive formulas for $q(RD^{(1)})$, $q(RD^{(2)})$, and $q(RD^{(1)}{}_2)$ that take into account the S−R interactions. In appendix B, we generate expressions for the binding constants (K's) based on the q's. These are given in the fourth column of Table S1 of the Supporting Information.

2.3. Binding Efficiency of Bivalent Complex. The quantity typically employed as a measure of the potency of the ligand to induce a desired effect is EC_{50}, which is the effective concentration of the ligand needed to induce one-half the maximum effect. Equivalently, $EC_{50} = [D]_{1/2}$ is the concentration of the ligand D when the following condition holds:

$$[R]_{sat}/[R]_{all} = 1/2 \tag{1}$$

In eq 1, $[R]_{sat}$ stands for the total concentration of all saturated complexes (i.e., both binding sites of R are occupied by ligating units) and $[R]_{all}$ for the total concentration of all species involving R (i.e., including also Rs with unoccupied sites). In preceding work[12,13] following Hill,[38] we invoked the "all-or-none" hypothesis to simplify the theoretical treatment, as well as to be in accord with the analysis of experimental data,[14] which is also based on it. The all-or-none hypothesis, which assumes that either all sites of a given R are occupied by ligating units at once or none of the sites is occupied, is equivalent to ignoring the role of complexes of intermediate degrees of saturation.

In this Article, we eschew the all-or-none simplification. Hence, for the binding of bivalent D to bivalent R, eq 1 can be written explicitly:

$$\frac{[RD_2^{(1)}] + [RD^{(2)}]}{[R] + [RD^{(1)}] + [RD_2^{(1)}] + [RD^{(2)}]} = \frac{1}{2} \tag{2}$$

dx.doi.org/10.1021/jp211383s | J. Phys. Chem. B 2012, 116, 2595−2604

In terms of the overall binding constants $K(\mathrm{X})$ of the complexes X, we can recast eq 2 as

$$K(\mathrm{RD}_2^{(1)})[\mathrm{D}]_{1/2}^2 + \{K(\mathrm{RD}^{(2)}) - K(\mathrm{RD}^{(1)})\}[\mathrm{D}]_{1/2} - 1 = 0 \quad (3)$$

where $[\mathrm{D}]_{1/2} = \mathrm{EC}_{50}$ is the concentration at which the R's are 50% saturated. Substituting theoretical expressions for the K's, which now account for molecular symmetry, and solving the resulting quadratic equation, we obtain:

$$[\mathrm{D}]_{1/2} = \frac{1}{4\nu_M\eta_1}\left[2 - \nu_M C_{\mathrm{eff}}(R)\eta_2\eta_1^{-1} + \sqrt{(2 - \nu_M C_{\mathrm{eff}}(R)\eta_2\eta_1^{-1})^2 + 4}\right] \quad (4)$$

In eq 4, $C_{\mathrm{eff}}(R)$ is the effective concentration of the unbound ligating unit of D at distance R from the other unit bound to a site of R (see eq B.6 of the Supporting Information); ν_M stands for the effective volume available to a ligating unit bound in a site of R (see eq A13a). The quantities $\eta_j \equiv \langle \exp(-U^{(\mathrm{SR})}/k_BT)\rangle_j$ (where k_B is Boltzmann's constant and T is the absolute temperature) are averages of the Boltzmann factor over subensembles (designated by index j) of conformations of the free S-chain restricted so that either one ligating unit ($j = 1$) or both units ($j = 2$) of the same D are bound to R (see eqs B7 and B9).

In the limit of short S-chains, when $C_{\mathrm{eff}}(R) \to 0$, because the second unit of D cannot bind to the other site of R, and $\eta_1 \to 1$, because S−R interactions become negligible, eq 4 simplifies to

$$[\mathrm{D}(C_{\mathrm{eff}} = 0)]_{1/2} = (1 + 2^{1/2})/(2\nu_M) \quad (5)$$

Given the value of $[\mathrm{D}(C_{\mathrm{eff}} = 0)]_{1/2}$ in eq 5, one can estimate the value of ν_M, an important parameter characterizing the binding of the ligating unit to R. If the all-or-none hypothesis is invoked, as in our previous works,[12,13] eq 5 reads either $[\mathrm{D}(C_{\mathrm{eff}} = 0)]_{1/2} = 1/\nu_M$ if symmetry numbers are ignored, or $[\mathrm{D}(C_{\mathrm{eff}} = 0)]_{1/2} = 1/(2\nu_M)$ if symmetry numbers are included (see Table S2 in the Supporting Information). Hence, refraining from the all-or-none assumption and accounting for molecular symmetry yields a value of ν_M larger by a factor of $(1 + 2^{1/2})/2 \approx 1.2$ than the value used earlier[12,13] by invoking the all-or-none hypothesis and neglecting molecular symmetry.

Because the synthesis of very short PEG chains bound to cGMP is impractical, $[\mathrm{M}]_{1/2}$ was measured for RET[14] and used instead of $[\mathrm{D}(C_{\mathrm{eff}} = 0)]_{1/2}$. The two concentrations can be related by noting that D carries two ligating units and is therefore twice as efficient at binding as M (equivalent to a single unit) at the same concentration, in the limit of very short S-chains. Hence, we have

$$[\mathrm{D}(C_{\mathrm{eff}} = 0)]_{1/2} \equiv [\mathrm{M}]_{1/2}/2 \quad (6)$$

which we take as the formal reference value of $[\mathrm{D}(C_{\mathrm{eff}} = 0)]_{1/2}$ for vanishing S-chain length. Therefore, to obtain a realistic estimate of the parameter ν_M, we use for RET the value $[\mathrm{D}(C_{\mathrm{eff}} = 0)]_{1/2} = 36\ \mu\mathrm{M}$ rather than the value 72 μM that was estimated by Kramer and Karpen[14] and used by us previously.[12,13] With $[\mathrm{D}(C_{\mathrm{eff}} = 0)]_{1/2} = 36\ \mu\mathrm{M}$ and the minimum value $[\mathrm{D}]_{1/2}(\mathrm{min}) = 0.4\ \mu\mathrm{M}$, measured for RET,[14] the maximum enhancement effect is $[\mathrm{D}(C_{\mathrm{eff}} = 0)]_{1/2}/[\mathrm{D}]_{1/2}(\mathrm{min}) = 90$ rather than 180.

3. MODELS AND METHODS

3.1. Receptor. In light of the enormous variety and complexity of real molecular systems and lack of structural knowledge of the ligand−receptor complex for which experimental measurements of EC_{50} are available, we refrain from specifying atomic details and rather tailor a model of R with a few essential features that may characterize a broad class of multivalent Rs. We suppose R to possess a smooth surface (impenetrable to S-chain atoms) comprising hills (or depressions) with the binding sites on top (or at the center) (see Figure 1). Far from the peaks of the hills, the surface tends to a basal plane that extends formally to infinity, so that the effect of the membrane in which R is embedded is included. The topography between the sites is then either concave or convex, if the sites are on the peaks of the hills or at the centers of the depressions, respectively. For example, RET, a homotetrameric protein complex whose sites are located on each of the four monomers that surround a central ion channel, likely exhibits a concave topography (i.e., the entrance to the ion channel is in a valley created by the surrounding proteins; see Figure 1 of ref 14).

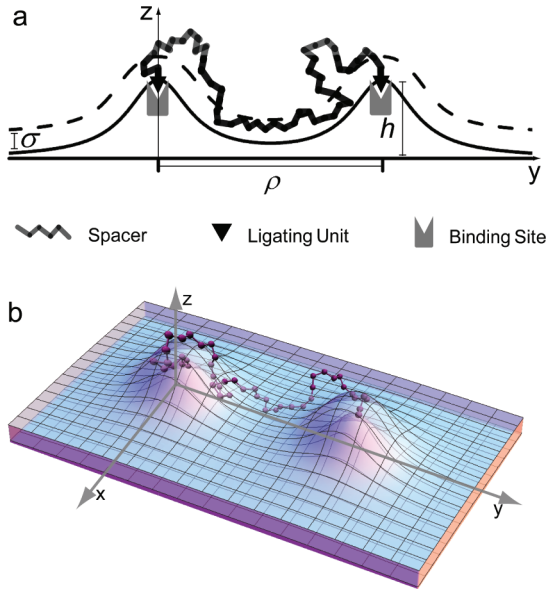

Figure 1. (a) Schematic side view of bivalent receptor ($\mathrm{R}_{\mathrm{hard}}$) with binding sites occupied by ligating units of bivalent ligand connected by polymeric spacer. Hard surface of R defined by function $z = H_{\mathrm{hard}}(x, y)$, eq 7 ($\rho = 30$, $h = 10$ Å), where h is height and ρ is the distance between two Lorentzian hills (of 0.25 ρ half width at half height) on top of which are binding sites. Function H_{hard} represents the distance from the hard surface of receptor to the basal x−y plane. Second surface (H_{soft}, dashed line) bounds range of distances $H_{\mathrm{hard}} < z < H_{\mathrm{soft}}$ over which atoms of S may be subject to attractive square well of fixed width $\sigma = 2b = 3.06$ Å and variable depth W. (b) Three-dimensional perspective of R surface concave between binding sites. Displayed are H_{hard} (solid) and H_{soft} (transparent) with bivalent ligand D (including S-chain) bound to binding sites located on the tops of two Lorentzian hills.

We assume the two hills (depressions) carrying the binding sites possess cylindrical symmetry with Lorentzian profiles of height $h > 0$ (depth, $h < 0$) and full width at half height of 0.25 ρ, where ρ is the distance of the two sites. We take the origin of the coordinate system to be in the basal x−y plane of R and the z axis to coincide with the axis of the hill bearing site α (see

dx.doi.org/10.1021/jp211383s | J. Phys. Chem. B 2012, 116, 2595−2604

Figure 1a). Thus, the two sites α and β are located at $\mathbf{r}_\alpha = h\mathbf{e}_z$ and $\mathbf{r}_\beta = \rho\mathbf{e}_y + h\mathbf{e}_z$, respectively, where $\mathbf{e}_x$, $\mathbf{e}_y$, and $\mathbf{e}_z$ are Cartesian unit vectors. Hence, the surface of R is specified by the locus of points $\mathbf{r} = (x, y, z)$ fulfilling the condition:

$$z = H_{\text{hard}}(x, y) = H_\alpha(x, y) + H_\beta(x, y) \tag{7a}$$

where

$$H_\lambda(x, y) = h\rho^2/[\rho^2 + 16x^2 + 16(y - y_\lambda)^2]$$

$$y_{\lambda=\alpha} = 0, \quad y_{\lambda=\beta} = \rho \tag{7b}$$

We designate this model as R_{hard}.

3.2. Polymeric Spacer, Bivalent Ligand, and Ligand–Receptor Complex. Several of the key experiments on multivalent ligand binding employ PEG chains as spacers.[14,16,25,26] A PEG chain (S-chain) comprising N_M monomers can be represented by the formula H $(O-CH_2-CH_2)_{N_M}$–OH. The bivalent ligand D is constructed by covalently bonding the end atoms of the S-chain to the monovalent ligands M. A ligating unit binding to R is considered to be buried in the binding site, such that the corresponding end atom of the S-chain is constrained to the top of the hill bearing that site. Thus, $RD^{(1)}$ is constructed by fixing one end atom of the S-chain at position $\mathbf{r}_\alpha = h\mathbf{e}_z$ where site α is situated; $RD^{(2)}$ is constructed by fixing also the second end atom of the S-chain at site β at position $\mathbf{r}_\beta = \rho\mathbf{e}_y + h\mathbf{e}_z$ (see Figure 1a). We model the PEG chain as a freely jointed chain of $3N_M + 1 = N_S$ identical concatenated beads that represent the O atoms and CH_2 groups of PEG. The C–C and O–C covalent bonds of the PEG chain are taken to be equivalent and of the same length $b = 1.53$ Å.

3.3. Spacer–Receptor Interaction. Assuming that all non-hydrogen atoms (beads) of S interact independently with R according to the same potential ψ, we can express the S–R interaction as the sum:

$$U^{(\text{SR})}(\mathbf{r}_1, \mathbf{r}_2, \ldots \mathbf{r}_{N_S}) = \sum_{i=1}^{N_S} \psi(\mathbf{r}_i) \tag{8}$$

The potential energy $\psi(\mathbf{r}_i)$ of interaction of the ith atom of S with R is given by

$$\psi(\mathbf{r}_i) = \begin{cases} \infty, & z_i \le H_{\text{hard}}(x_i, y_i) \\ -W, & H_{\text{hard}}(x_i, y_i) < z_i \le H_{\text{soft}}(x_i, y_i) \\ 0, & z_i > H_{\text{soft}}(x_i, y_i) \end{cases} \tag{9}$$

where $z = H_{\text{hard}}(x, y)$, eq 7a, describes the impenetrable "hard" surface of R. In a distance range $H_{\text{hard}} < z \le H_{\text{soft}}$ defined by a second, "soft" surface H_{soft} close to the hard surface, the atoms of the S-chain may be weakly attracted to R. Such an attractive region, modeled here as a square well, can account for potential hydrophobic interactions between S and R. To generate the soft surface of R, a sphere of radius $\sigma = 2\ b$ (b is the bond length between atoms of the S-chain) is rolled over the hard surface of R (see Figure S1 of the Supporting Information). The locus of the center of the rolling sphere defines the soft surface. This procedure is commonly applied to proteins to define the solvent-accessible surface area (SASA).[39,40] A simple rolling-sphere algorithm can be employed if the protein volume is defined by a discrete number of atoms.[41] In the present application, we use a different algorithm, storing the computed values of $H_{\text{soft}}(x, y)$ on a rectangular grid (see appendix C of the Supporting Information for details).

In this study, we consider three different R models for the S–R interaction: (1) the hard R model (R_{hard}) with a hard wall only ($W = 0$) and different topologies of the R surface (variable h), (2) the planar R model (R_{planar}) ($h = 0$) with attractive square well potential (variable W), and (3) the nonplanar "soft" R model (R_{soft}) ($h > 0$) with attractive S–R interactions (variable W), eq 9.

3.4. Computation of Effective Concentration C_{eff} and Ensemble Averages η_j. The quantity of primary interest, EC_{50}, itself depends on $C_{\text{eff}}(R)$ and η_j, whose computation requires knowledge of the probability distribution (density) function of the free S-chain. This distribution is represented by an ensemble of N_{ens} conformations of the S-chain, each of which is generated by a continuous random walk comprising $N_S - 1$ random flights, as detailed in appendix D of the Supporting Information.

For all models considered here, $U^{(\text{SR})} = \infty$ if $z_i < H(x_i, y_i)$ for any atom i of the S chain (see eq 9). Therefore, only those free S-chain conformations that do not penetrate the hard surface of R contribute to $\eta_j = \langle \exp(-U^{(\text{SR})}/k_BT)\rangle_j$. The subscript j denotes ensembles for two different situations: $j = 1$ corresponds to one end of the S-chain fixed on binding site α of R to form $RD^{(1)}$; $j = 2$ corresponds to both ends of the S-chain fixed on the sites of R to form $RD^{(2)}$. See appendix E of the Supporting Information for details.

To control statistical errors, which depend on the model, we employ ensembles of free S-chain conformations ranging from $N_{\text{ens}} = 5 \times 10^6$ to $N_{\text{ens}} = 10^{10}$. We estimate statistical errors roughly by using the first and second halves of the generated free S–chain conformations to evaluate η_1 and η_2. Deviations between the two halves larger than the width of the lines in the corresponding figures are indicated by error bars. The statistical errors are negligible in the absence of S–R attraction (Figure 2) but can become appreciable for long S-chains and large S–R attraction (Figure 4b).

4. RESULTS AND DISCUSSION

Our principal concern is to explore the impact of the S–R interactions on the stability of the bivalent ligand–receptor complex relative to its monovalent counterpart. For this purpose, we focus on EC_{50} (i.e., $[D]_{1/2}$). According to eq 4, $[D]_{1/2}$ depends on ν_M, the effective interaction volume available for a ligating unit in the binding site, $C_{\text{eff}}(R)$, the effective concentration of one ligating unit of D when the other unit is bound to one of the two sites of R as well as on η_1 and η_2. The ensemble averages η_1 and η_2 depend, according to eq B9 of the Supporting Information, on $U^{(\text{SR})}$, which in turn is determined by the model of R (i.e., either R_{hard}, R_{planar}, or R_{soft}), as described in section 3. We estimate a typical value of the effective interaction volume ν_M available for a ligating unit in the binding site of R from experimental data, rather than modeling the binding interaction of a ligating unit with R. In particular, we employ data of Kramer and Karpen on the binding of cGMP to RET.[14] Hence, we set $T = 300$ K, $\rho = 30$ Å, and $\nu_M \approx 0.0335\ \mu M^{-1}$. This estimate of the value of ν_M is based on the measured value of $[M]_{1/2} = 72\ \mu M$.[14]

Equation 4 can be rewritten as $[D]_{1/2} = (4\nu_M\eta_1)^{-1}\{2 - q + [(2 - q)^2 + 4]^{1/2}\}$, where

$$q = \nu_M C_{\text{eff}}\eta_2/\eta_1 \tag{10}$$

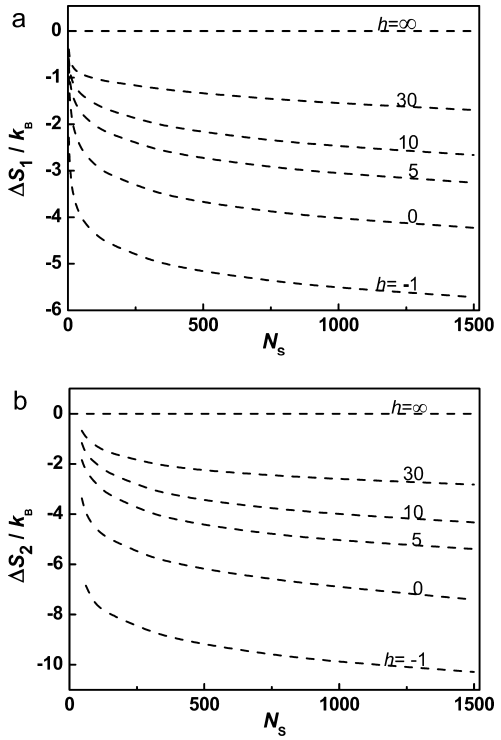

Figure 2. (a) Entropy loss ΔS_1 (equivalent to free energy difference $-\Delta F_1 = T\Delta S_1$) due to S−R interaction $U^{(SR)}$ on binding of one ligating unit of D to R, as a function of S-chain length (in number of atoms N_S) for hard receptor model (R_{hard}) with different heights h [Å] of Lorentzian hills ($h = -1$, 0, 5, 10, 30, ∞). $h = -1$ Å corresponds to Lorentzian depressions of depth 1 Å; $h = \infty$ corresponds to the absence of S−R interaction. Distance between binding sites is $\rho = 30$ Å. $\Delta S_1/k_B = \ln(\eta_1)$ is computed over an ensemble of between 3×10^{10} and 3×10^{11} conformations of free S-chains, constrained so that one end atom is fixed at binding site α of R. Ensemble average $\eta_1 = \langle \exp(-U^{(SR)}/k_BT)\rangle_1$ is equivalent to fraction of S-chain conformations for which all atoms lie above H_{hard}, eq 7 (see Figure 1). (b) Entropy loss ΔS_2 (equivalent to free energy difference $-\Delta F_2 = T\Delta S_2$) due to S−R interaction on binding of both ligating units of D to R, as function of S-chain length (in number of atoms N_S) for R_{hard} model. Ensemble average $\eta_2 = \langle \exp(-U^{(SR)}/k_BT)\rangle_2$ [yielding $\Delta S_2/k_B = \ln(\eta_2)$] is over conformations of free S-chains constrained so that end atoms are fixed at binding sites of R. Same notation and parameters as in (a).

Thus, $[D]_{1/2}$ manifests two dependences on ν_M through the prefactor ν_M^{-1} and the parameter $q(\nu_M)$ ($q \geq 0$). The inverse proportionality to ν_M reflects monovalent binding in the absence of multivalency (i.e., the binding to R of ligating units from different D's). The enhancement effect of multivalent binding depends crucially on $q(\nu_M)$. It is the key parameter governing the efficiency of multivalent binding with flexible spacers. If monovalent binding is too weak (i.e., ν_M is small), there is no enhancement effect. Indeed, as indicated in Figure S3 of the Supporting Information, an appreciable enhancement effect is possible only if q is much greater than 2. Hence, in this regime of q, which corresponds to the minimum of the plot of $[D]_{1/2}$ versus the Flory radius R_F (root-mean-square end-to-end distance of the S-chain, defined by eq D3 of the Supporting Information), an increase in ν_M results in an increase in enhancement effect. Accordingly, the estimate of ν_M that we now use, which is a factor of ~1.2 larger than that of ν_M employed in our earlier work,[12,13] leads to a substantial increase in the enhancement effect.

The parameter $q(\nu_M)$ [eq 10] is proportional to ν_M by the factor $C_{eff}\eta_2/\eta_1$. It reflects the binding of the second ligating unit of D to R. C_{eff} describes the essence of the enhancement effect (i.e., the enhanced concentration of the second unit of a D whose first unit is already bound to R). The ratio η_2/η_1 describes how the S−R interactions modulate the enhancement effect. It is generally smaller than unity, thus diminishing the enhancement effect appreciably. However, as demonstrated below, the ratio η_2/η_1 grows with increasing concavity of the R surface and attraction between S and R.

We stress that the ensemble averages η_j are the sole parameters of the model that reflect the influence of the S−R interaction on the enhancement effect, as measured by EC_{50}. It is shown in appendix G of the Supporting Information that the contribution of the S−R interaction to the free energy of binding for $RD^{(j)}$ is $\Delta F_j = -k_BT \ln(\eta_j)$ for $j = 1, 2$.

4.1. Strictly Repulsive Surface R_{hard}: Variation of Height of Hills. We examine first the dependence of η_j on the height (depth) (h) of the two hills (depressions) of R_{hard} (see eq 7). Hence, $\Delta F_j = -T\Delta S_j$, where $\eta_j = \exp(\Delta S_j/k_B)$ (see appendix G of the Supporting Information) is just the fraction of conformations of the S-chain for which all beads lie above the hard surface of R ($z = H_{hard}(x,y)$). Accordingly, ΔS_j is the loss of entropy of the free S-chain of D due to its interaction with R, as the j (=1,2) ligating units bind to the sites to form $RD^{(j)}$.

Figures 2a and b display plots for R_{hard} of $\Delta S_1/k_B$ and $\Delta S_2/k_B$ versus S-chain length (N_S) for several heights h of the hills. The horizontal lines ($h = \infty$, $\Delta S_j = 0$) correspond to the absence of S−R interactions, as assumed in our prior work.[12,13] As h decreases, the entropy loss increases markedly for both complexes $RD^{(1)}$ and $RD^{(2)}$. Note, however, that the rate of entropy loss for $RD^{(2)}$ is nearly twice that for $RD^{(1)}$, because fewer free S-chain conformations survive the requirement that all atoms lie above $H_{hard}(x, y)$ when both ends of the S-chain are bound to the sites of R. We note in passing that the dependence of η_j on N_S approximately obeys a power law $\eta_j = \exp(\Delta S_j/k_B) \approx (N_S)^{-j/2}$ as $N_S \rightarrow \infty$ (see Figure S2 of the Supporting Information). For $j = 1$, the corresponding power law was previously reported for a polymer chain with one end attached to a planar hard wall.[42]

We conclude that the hard surface of R engenders strong decreases in the entropy of the S-chain as D binds to R. For positive h, the landscape of R between the two binding sites is concave. With decreasing h, the concavity becomes weaker and the entropy loss stronger. The entropy loss becomes dramatically large if R possesses a convex landscape ($h < 0$). Thus, the decrease in entropy as h goes from 0 to −1 is approximately equal to that as h goes from 10 to 0 (see Figure 2).

This entropy loss gives rise to lower stability of the complexes. Plots of $[D]_{1/2}$ versus the Flory radius R_F demonstrate this effect (see Figure 3). As the height h of the hills decreases, the entropy loss of the S-chain increases and $[D]_{1/2}$ rises correspondingly (Figure 3). For short S-chains (i.e., small R_F), where the second ligating unit is still unable to bind, $[D]_{1/2}$ increases with increasing R_F because of the entropy loss of the S−chain due to its interaction with the R surface. Likewise, for long S-chains (i.e., large R_F), $[D]_{1/2}$ increases again, because C_{eff} decreases. At intermediate R_F, $[D]_{1/2}$ goes through a minimum, and the enhancement effect is maximal here. The minimum in $[D]_{1/2}$ is deeper for the measured than for the computed $[D]_{1/2}$.

dx.doi.org/10.1021/jp211383s | J. Phys. Chem. B 2012, 116, 2595−2604

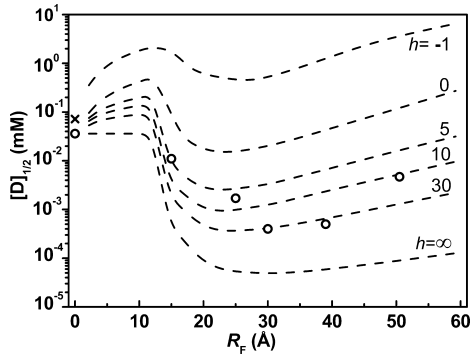

Figure 3. $[D]_{1/2}$ for binding of D to R for R_{hard} model, as a function of Flory radius R_F (root-mean-square end-to-end distance for free ligand D, eq D3) of S-chain for different heights of Lorentzian hills (h = −1, 0, 5, 10, 30, ∞), eq 7. Results correspond to those of Figure 2a and b. "○" refer to experimental data on activation of RET.[14] Distance between binding sites fixed at ρ = 30 Å, as suggested in ref 14. Symbol "×" at R_F = 0 marks measured value $[M]_{1/2}$ = 72 μM for monomeric cGMP.[14] Reference value for limiting concentration (open circle at R_F = 0) is $[D(C_{eff} = 0)]_{1/2}$ = 36 μM. Curve labeled h = ∞ refers to previously proposed model,[12,13] where we neglected the S−R interactions and applied the all-or-none hypothesis.[38] Note, however, in contrast to the preceding study, we consider here bivalent instead of tetravalent R.

In the absence of the S−R interaction (h = ∞), the computed minimum of $[D]_{1/2}$ is significantly below the minimum of the measured $[D]_{1/2}$ and located exactly at R_F = ρ = 30 Å corresponding to the estimated distance[14] between the two binding sites. However, with increasing S−R interaction (smaller h), the minimum of $[D]_{1/2}$, albeit shallow, shifts to smaller R_F values (Figure 3). Although the curve of $[D]_{1/2}$ in Figure 3 labeled h = ∞ is based on the model with vanishing S−R interaction,[12,13] the enhancement effect is now considerably larger, because the present estimated value of ν_M, which avoids the all-or-none hypothesis and accounts for molecular symmetry, is greater than the previous one by a factor of 1.2. Thus, room is available for additional modifications of the present model that may diminish the enhancement effect. For the planar R surface (h = 0 Å), the enhancement is negligibly small, while for R with weakly convex surfaces (h = −1 Å), binding of D becomes dramatically hampered as compared to binding of M (see Figure 3).

As Figure 3 indicates, we need pronounced concavity of the R landscape with hill heights of at least h = 10 Å to qualitatively describe the enhancement measured for the activation of RET.[14] If we wanted to reproduce the measured maximum enhancement of $[D(C_{eff} = 0)]_{1/2}/[D]_{1/2}(min)$ = 90, according to Figure 3, we would need to set $h \approx$ 30 Å, which may be unreasonably large. Therefore, we consider other options, weak attractive interactions of the PEG chain with the protein R surface.

4.2. Spacer−Receptor Attraction: R_{planar} and R_{soft} Models. If the spacer material were strictly hydrophilic, there would be no attraction between S and R. However, there are strong indications that PEG is not perfectly hydrophilic. PEG chains generally repel proteins by loss of conformational entropy, as long as the PEG−protein interface is relatively small. As this interface grows, weak hydrophobic and van der Waals attractions between PEG and protein may become significant.[31−35] Several independent lines of evidence point to the ability of PEG to attract nonpolar as well as polar regions of proteins.[36] When PEG is used to foster crystallization of proteins, it may be observed in the crystal structures. For example, structurally ordered PEG chains have been found inside the ion channel of OmpF porin.[37] Such attractive interactions of PEG with protein surfaces were also observed for the cGMP activated ion channels.[14] For RET, it was observed that monomeric cGMP with attached PEG chain binds as efficiently as the bare cGMP monomer, despite the entropy loss that a PEG chain experiences in the neighborhood of the R surface. For the olfactory ion channel, the monomeric cGMP with attached PEG chain binds to the receptor even more efficiently than does the bare monomeric cGMP.[14] On the basis of these experimental results, we may conclude that the entropy loss of the PEG chain upon binding of cGMP is compensated by attractive interactions between the PEG chain and the surface of RET.

Therefore, such strictly repulsive R models as R_{hard} may be unrealistic in that they do not account for the weak attractive forces that come into play as the S-chain approaches the surface of R. To explore the influence of an attractive contribution to the S−R interaction, we employ first a simple R model (R_{planar}) consisting of a hard plane with an attractive square well potential (width σ and depth W) next to it. We vary the well depth W and fix the width to σ = 2b = 3.06 Å, which roughly corresponds to the thickness of a single atomic layer at the R surface. Implicit solvent models of solutes in water mimic the hydrophobic effect[43] usually by a surface energy term whose of strength varies from 0.012 kcal/(mol Å^2) for small molecules[44,45] to 0.030 kcal/(mol Å^2), a value used for proteins.[46,47] The hydrophobic effect acting on a solute (in our case receptor and spacer) is proportional to the SASA of the solutes. Taking the radius of the atoms of the S-chain to be b = 1.53 Å, we estimate the effective decrease in SASA for one atom of S in contact with the R surface to be $2\pi b^2$ = 14.7 Å^2. Thus, we estimate that when one atom of the hydrophobic S is in contact with the protein R surface, its free energy decreases by about W = 0.44 kcal/mol. Because PEG is only weakly hydrophobic, the decrease in free energy should be much smaller. We indeed find that values of W an order of magnitude smaller than this estimate are large enough to explain the experiments.

In Figures 4a and b are plotted $\ln(\eta_1) = -\Delta F_1/(k_BT)$ and $\ln(\eta_2) = -\Delta F_2/(k_BT)$ as functions of the S-chain length (N_S) for the R_{planar} model for several well depths W at fixed well width σ = 2b = 3.06 Å corresponding to two bond lengths of S. The curves labeled W = 0.000 in Figures 4a and b correlate with those in Figures 2a and b labeled 0 (h = 0). As the well gets deeper, $-\Delta F_j$ fall off more slowly with increasing N_S, eventually becoming almost flat at W = 0.045 kcal/mol, where enthalpy gain compensates entropy loss over a large interval of N_S. This condition likely corresponds to the experimental observation that the binding to RET is for monovalent cGMP with an attached PEG chain as efficient as for a bare cGMP.[14] In fact, this value of W is about 10 times smaller than the above estimate of 0.44 kcal/mol for the free energy of association of an atom of a strongly hydrophobic molecular species with a protein surface.

For the R_{planar} model, the influence of the attractive part of the S−R interaction on the enhancement effect is demonstrated in Figure 5, which shows plots of $[D]_{1/2}$ versus Flory radius R_F that correspond to those of Figure 3. According to our expectation, $[D]_{1/2}$ decreases as the attractive square well deepens, such that at W = 0.045 kcal/mol the enhancement

dx.doi.org/10.1021/jp211383s | J. Phys. Chem. B 2012, 116, 2595−2604

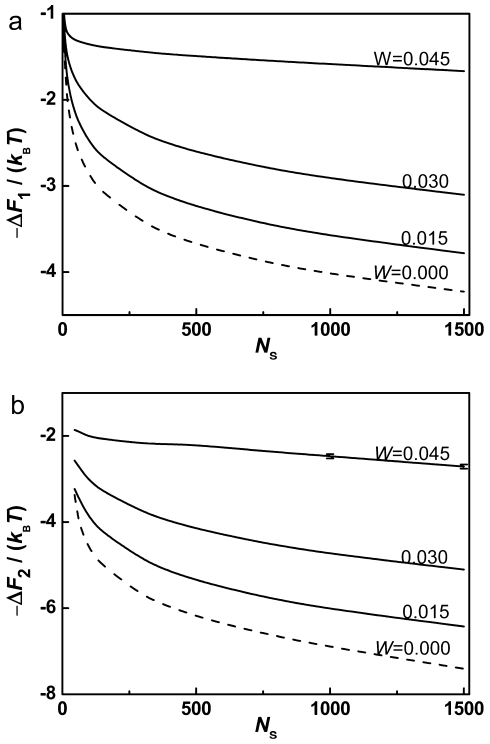

Figure 4. (a) Change in (negative) free energy due to S−R interaction on binding of one ligating unit of bivalent ligand to bivalent R for R_{planar} model (h = 0), as a function of S-chain length (in number of atoms N_S). S−R interaction is modeled by attractive square well potential next to the R surface. Well depth W [kcal/mol] varies between 0.0 and 0.045. Distance between binding sites is ρ = 30 Å. (b) Change in (negative) free energy due to S−R interaction on binding of both ligating units of bivalent ligand to bivalent R, as a function of S-chain length. Error bars shown where the statistical error is larger than line width (i.e., for W = 0.045 at large N_S). Same R_{planar} model, notation, and parameters as in (a).

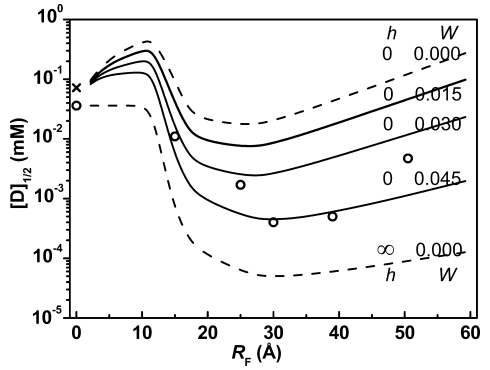

Figure 5. $[D]_{1/2}$ of binding of D to R, as a function of the Flory radius R_F for the R_{planar} model with different well depths W [kcal/mol]. Results correspond to those of Figure 4a and b. Dotted reference curves labeled h = 0 and h = ∞ with W = 0.0 are reproduced from Figure 3. "○" refer to experimental data on RET.[14]

becomes as large as the maximum enhancement of $[D(C_{eff} = 0)]_{1/2}/[D]_{1/2}(min)$ = 90 measured for RET. Furthermore, this value of W coincides with the value for which the monovalent ligand with an attached polymer chain binds as efficiently to R as M alone. See Figure 4a, which shows that $-\Delta F_1$ nearly vanishes and does not substantially change with the S-chain length. This agrees with measurements on the binding of cGMP to RET.[14]

In the R_{soft} model, we combine both concavity and S−R attraction so as to make the enhancement agree with that experimentally observed for RET. In Figure 6, we show the

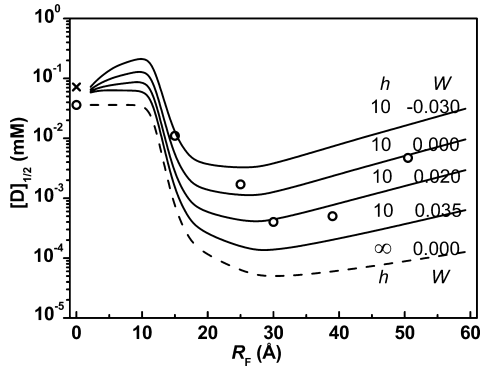

Figure 6. $[D]_{1/2}$ of binding of D to R, as a function of the Flory radius R_F for the R_{soft} model with different well depths W [kcal/mol] and fixed height h = 10 Å of Lorentzian hills, eq 7. Negative well depths correspond to S−R repulsion. Dotted reference curve labeled h = ∞ and W = 0.0 reproduced from Figure 3. "○" refer to experimental data on activation of RET.[14]

dependence of $[D]_{1/2}$ on Flory radius R_F for different well depths W with a fixed, moderate concavity of the R surface (h = 10 Å, depicted in Figure 1a). For this degree of concavity, an even smaller S−R attraction of W = 0.020 kcal/mol yields an enhancement $\{[D(C_{eff} = 0)]_{1/2}/[D]_{1/2}(min)\}$ as large as that measured for RET[14] (Figure 6). We can conclude that even a very small attractive S−R component corresponding to weak hydrophobicity can lead to a large enhancement effect in multivalent ligand binding.

5. CONCLUSIONS

Properly designed multivalent ligands combined with appropriately chosen multivalent receptors bind often by orders of magnitude more efficiently than their monovalent analogs.[14−29] A prime example is the binding of polymer-linked bivalent ligands (cGMP moieties connected by PEG chains) to tetravalent receptors such as RET.[14] The increase in efficiency of multivalent binding is rationalized in terms of the "effective concentration" (C_{eff}) of ligating units. If some units of the multivalent ligand are already bound to R, the effective concentration of the remaining unbound ligating units at the unoccupied binding sites of R can be much greater than that of free ligands in solution. Thus, for a bivalent ligand, it is more probable that the second unit binds to an available site of the same R than that another ligand binds from solution. A simple model[12,13] incorporating this concept was able to explain semiquantitatively the measured dependence of EC_{50} ($[D]_{1/2}$) on the length of the PEG S−chain.

For the sake of simplicity, the S−R interaction was neglected in our earlier studies on bivalent binding.[12,13] The present work includes these interactions. To the best of our knowledge, preceding theoretical investigations on multivalent binding ignored S−R interactions, except for one very recent study.[30] Furthermore, we refrain here from invoking Hill's simplifying all-or-none assumption,[38] which ignores the semisaturated ligand−receptor complex $RD^{(1)}$, where one binding site is occupied, while the second site is empty. Avoiding the all-or-

dx.doi.org/10.1021/jp211383s | J. Phys. Chem. B 2012, 116, 2595−2604

none assumption and accounting for molecular symmetry increases the enhancement effect of bivalent binding by more than an order of magnitude, leaving room for additional factors in improved models that may reduce enhancement. In fact, the S−R interaction, absent in previous studies, has a strong influence and can reduce the efficiency of multivalent ligand binding substantially. Furthermore, we have shown that the enhancement effect of bivalent binding with a flexible spacer is governed by a single parameter q [see eq 10]. The dependence of this parameter on monovalent binding efficiency (ν_M), effective concentration (C_{eff}), and S−R interactions provides guidelines for the design of bivalent ligand−receptor complexes that can exhibit strong enhancement. We believe that such guidelines can also be extended to more general cases of multivalent binding.

The R with a hard surface (R_{hard} model) forces the atoms of S to stay outside of R, thus diminishing the number of allowed S-chain conformations and dramatically lowering the S-chain entropy (or, equivalently, increasing the free energy) as the S-chain approaches the surface of R. As a consequence, the enhancement effect can be reduced by several orders of magnitude, even to the point of rendering the binding of monomeric ligands (M) more efficient than that of bivalent ligands. The reduction of the enhancement effect by S−R interaction is most pronounced for convex R surfaces, very large for planar R surfaces, and still significant for concave R surfaces. Only for unreasonably large concavity of the R surface is the computed enhancement sufficiently large to explain that seen for RET.[14] Hence, an attractive component of the S−R interaction is necessary to understand efficient bivalent binding for such complexes.

If an attractive layer next to the hard surface of R is included, the enhancement effect becomes larger again. Already, a weak S−R attraction only one tenth the magnitude of that between hydrophobic aliphatic carbon atoms can restore the enhancement for the planar R surface (R_{planar} model) to the value obtained in the absence of S−R interaction and thus reproduce the measured enhancement for the binding of bivalent cGMP to RET.[14] If concavity of R is combined with S−R attraction, a moderate concavity and very small S−R attraction is also sufficient to explain the enhancement effect of bivalent binding. In fact, there are a number of indications that PEG has a tendency to attach to protein surfaces and therefore may be slightly hydrophobic. The monomeric cGMP binds to RET with the same efficiency with and without an attached PEG chain,[14] which corroborates this behavior. Hence, the bivalent binding of cGMP to RET goes along with conformational entropy loss and gain of binding enthalpy of the spacer due to weak S−R interactions. These two contributions to binding free energy approximately compensate for concave receptor topography. That is why simplified earlier theoretical models of bivalent ligand binding that ignored the S−R interaction were able to provide fortuitous agreement with the measurements for these systems. Such compensation between entropy and binding enthalpy may hide the influence of S−R interactions on multivalent binding also for other systems.

A depression, or valley, between the binding sites of R, as depicted in Figure 1, results in a concave R surface. This topography is likely not widespread in the universe of protein structures. In fact (based on a preliminary scan, work in progress), bivalent R's that possess a concave surface between the two ligand binding sites are scarce in the protein data bank.[48] Prominent examples of such receptors with concave topography[49] are the homo- and heterodimeric 14−3−3 proteins,[50] which are essential for signaling in all eukaryotes and appear also in plants.[51] Figure 7 depicts the concavity of

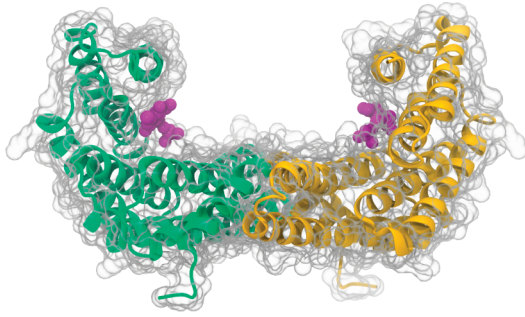

Figure 7. Concave R-surface between the two binding sites of the bivalent 14−3−3 dimeric receptor (PDB id 3RDH) pictured binding two FOBISIN101 ligands (magenta).[52] The backbones of the two polypeptides are traced by rubber bands in green and yellow. The transparent gray shaded area pictures the protein volume including the side chains.

the R-surface between the two sites of a bivalent 14−3−3 protein homodimer (PDB id 3RDH), which is shown to bind two drug-like molecules of a recently discovered inhibitor.[52] For artificial tandem peptide ligands involving phosphoserine, it was shown that binding to the 14−3−3 protein can be 30 times more efficient than for the monovalent correlates.[53] Recently, an artificial bivalent receptor was created by dimerizing carbonic anhydrase (CA).[54] The binding efficiency of bivalent sulfonamide ligands with this receptor (dime5rCA) was enhanced by up to a factor of 5000.[54] According to the crystal structures of dCA, the two binding sites are face-to-face corresponding to concave receptor topography, which is consistent with our results.

Another homodimeric receptor on which several bivalent ligand binding studies have been performed is the estrogen receptor (ER).[55,56] The topography between the two binding sites of the dimeric ER is neither concave nor planar, but strongly corrugated as can be seen in Figure 8. As a

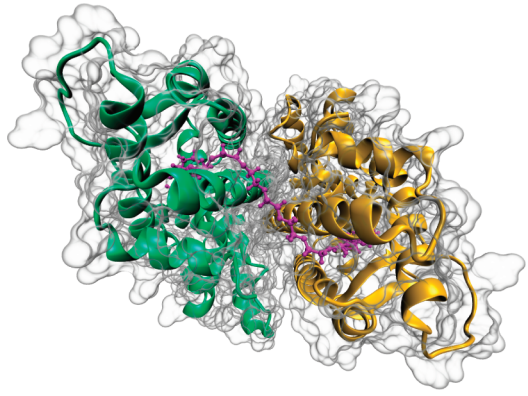

Figure 8. Corrugated R-surface between the two binding sites of the bivalent homodimeric estrogen receptor (ER), shown binding a bivalent ligand consisting of two diethylstilbestrol (DES) ligating units connected by a PEG spacer of 21 main-chain atoms. The spacer geometry is modeled on the basis of the ER crystal structure (PDB id 3ERD).[57] The PEG spacer needs to circumvent the two α-helices, which protrude from the ER surface. The same representation is used for the protein as for Figure 7.

dx.doi.org/10.1021/jp211383s | J. Phys. Chem. B 2012, 116, 2595−2604

consequence, the S-chain needs to form a bow to stay away from the ER surface or to adopt a complex nonlinear conformation that makes close contact between S and the ER surface. Hence, it is not surprising that several experimental attempts to produce an appreciable enhancement for the binding of bivalent ligands with flexible spacers have so far not been successful for this system.

In summary, the difficulties we encounter in the theoretical description of the binding of D to R with explicit S−R interactions may explain the paucity of experiments that successfully demonstrate an enhancement effect for bivalent complexes in which the spacer is flexible. Use of rigid spacers could be advantageous in cases where the topography of the receptor is not concave, although a major problem with rigid spacers is that they must be adroitly designed so as to be commensurate with the topography of the corresponding receptor. The influence of S−R interactions on multivalent ligand binding was so far mostly overlooked or considered to be negligibly small. In fact, its influence can abolish enhancement of binding or even yield bivalent binding affinities lower than in the monomeric case.

While the spacer−receptor models used in the present study are still based on very simplifying assumptions, they provide general guidelines for more detailed molecular models. For future work, it will be useful to perform simulations in atomic detail to enhance the understanding of multivalent binding. Computing the free energy of binding of a multivalent ligand to its receptor for such a detailed model requires molecular dynamics (MD) simulations of more than 10 000 atoms. For the present study, we needed up to 10^{10} independent spacer conformations generated by a Monte Carlo method to obtain precise enough data for the bivalent ligand binding. Assuming that an independent spacer conformation is generated after each picosecond of an MD simulation (actually a very optimistic guess), one would still need a trajectory of 10 ms duration to theoretically model the bivalent binding process with sufficient accuracy. Such MD simulations require an enormous amount of CPU time. To monitor spacer length dependencies as done in the present study, several such trajectories would be needed. To plan such expensive MD simulations, the present study can pave the way to choose the right conditions.

■ ASSOCIATED CONTENT

Supporting Information

Figures S1−S3, appendices A−G, and Tables S1−S3. This material is available free of charge via the Internet at http://pubs.acs.org.

■ AUTHOR INFORMATION

Corresponding Author

*E-mail: knapp@chemie.fu-berlin.de.

Notes

The authors declare no competing financial interest.

■ ACKNOWLEDGMENTS

We thank Tim Meyer for helping to prepare Figure 7. This work is supported by the collaborative research center SFB 765 project C1 from the Deutsche Forschungsgemeinschaft (DFG). D.J.D. thanks the science administration of the Freie Universität Berlin for travel grants.

■ ABBREVIATIONS

CA, carbonic anhydrase; cGMP, cyclic guanidine monophosphate; D, bivalent (or divalent) ligand; ER, estrogen receptor; *K*, binding constant; M, monomeric ligand; *q*, canonical molecular partition function; PEG, polyethylene glycol; R, bivalent receptor; $RD^{(1)}$, $RD^{(2)}$, and $RD_2^{(1)}$, complexes in which, respectively, one binding site of R is occupied by one ligating unit of D, both sites of R are occupied by units of a single D, and both sites are occupied by units of separate Ds; RET, nucleotide-gated ion channel in bovine rod photoreceptor cells; R_F, Flory radius (i.e., root-mean-square end-to-end distance between ligating units of free D); R_{hard} model, R model with hard surface; R_{planar} model, R model with planar surface and S−R attraction; R_{soft} model, R model with S−R attraction; S, spacer; SASA, solvent-accessible surface area

■ REFERENCES

(1) Huskens, J. *Curr. Opin. Chem. Biol.* **2006**, *10*, 537−543.
(2) Mammen, M.; Choi, S.-K.; Whitesides, G. M. *Angew. Chem., Int. Ed.* **1998**, *37*, 2754−2794.
(3) Kiessling, L. L.; Gestwicki, J. E.; Strong, L. E. *Angew. Chem., Int. Ed.* **2006**, *45*, 2348−2368.
(4) Collins, B. E.; Paulson, J. C. *Curr. Opin. Chem. Biol.* **2004**, *8*, 617−625.
(5) Joshi, A.; Vance, D.; Rai, P.; Thiyagarajan, A.; Kane, R. S. *Chem.-Eur. J.* **2008**, *14*, 7738−7747.
(6) Rolland, O.; Turrin, C.-O.; Caminade, A.-M.; Majoral, J.-P. *New J. Chem.* **2009**, *33*, 1809−1824.
(7) Mulder, A.; Huskens, J.; Reinhoudt, D. N. *Org. Biomol. Chem* **2004**, *2*, 3409−3424.
(8) Badjić, J. D.; Nelson, A.; Cantrill, S. J.; Turnbull, W. B.; Stoddart, J. F. *Acc. Chem. Res.* **2005**, *38*, 723−732.
(9) Schalley, C. A.; Lützen, A.; Albrecht, M. *Chem. Eur. J.* **2004**, *5*, 1072−1080.
(10) Baldini, L.; Casnati, A.; Sansone, F.; Ungaro, R. *Chem. Soc. Rev.* **2007**, *36*, 254−266.
(11) Martinez-Veracoechea, F. J.; Frenkel, D. *Proc. Natl. Acad. Sci. U.S.A.* **2011**, *108*, 10963−10968.
(12) Diestler, D. J.; Knapp, E. W. *Phys. Rev. Lett.* **2008**, *100*, 178101.
(13) Diestler, D. J.; Knapp, E. W. *J. Phys. Chem. C* **2010**, *114*, 5287−5304.
(14) Kramer, R. H.; Karpen, J. W. *Nature* **1998**, *395*, 710−713.
(15) Blaustein, R. O.; Cole, P. A.; Williams, C.; Miller, C. *Nat. Struct. Biol.* **2000**, *7*, 309−311.
(16) Loidl, G.; Groll, M.; Musiol, H.-J.; Huber, R.; Moroder, L. *Proc. Natl. Acad. Sci. U.S.A.* **1999**, *96*, 5418−5422.
(17) Kitov, P. I.; Sadowska, J. M.; Mulvey, G.; Armstrong, G. D.; Ling, H.; Pannu, N. S.; Read, R. J.; Bundle, D. R. *Nature* **1999**, *403*, 669−672.
(18) Fan, E.; Zhang, Z.; Minke, W. E.; Hou, Z.; Verlinde, C. L. M. J.; Hol, W. G. J. *J. Am. Chem. Soc.* **2000**, *122*, 2663−2664.
(19) Gargano, J. M.; Ngo, T.; Kim, J. Y.; Acheson, D. W. K.; Lees, W. J. *J. Am. Chem. Soc.* **2001**, *123*, 12909−12910.
(20) Zhang, Z.; Merritt, E. A.; Ahn, M.; Roach, C.; Hou, Z.; Verlinde, C. L. M. J.; Hol, W. G. J.; Fan, E. *J. Am. Chem. Soc.* **2002**, *124*, 12991−12998.
(21) Kitov, P. I.; Shimizu, H.; Homans, S. W.; Bundle, D. R. *J. Am. Chem. Soc.* **2003**, *125*, 3284−3294.
(22) Mulder, A.; Auletta, T.; Sartori, A.; Ciotto, S. D.; Casnati, A.; Ungaro, R.; Huskens, J.; Reinhoudt, D. N. *J. Am. Chem. Soc.* **2004**, *126*, 6627−6636.
(23) Trevitt, C. R.; Craven, C. J.; Milanesi, L.; Syson, K.; Mattinen, M.-L.; Perkins, J.; Annila, A.; Hunter, C. A.; Waltho, J. P. *Chem. Biol.* **2005**, *12*, 89−97.
(24) Farrera, J.-A.; Hidalgo-Fernández, P.; Hannink, J. M.; Huskens, J.; Rowan, A. E.; Sommerdijk, N. A. J. M.; Nolte, R. J. M. *Org. Biomol. Chem.* **2005**, *3*, 2393−2395.

(25) Krishnamurthy, V. M.; Semetey, V.; Bracher, P. J.; Shen, N.; Whitesides, G. M. *J. Am. Chem. Soc.* **2007**, *129*, 1312−1320.
(26) Shewmake, T. A.; Solis, F. J.; Gillies, R. J.; Caplan, M. R. *Biomacromolecules* **2008**, *9*, 3057−3064.
(27) Kane, R. S. *Langmuir* **2010**, *26*, 8636−8640.
(28) Huskens, J.; Mulder, A.; Auletta, T.; Nijhuis, C. A.; Ludden, M. J. W.; Reinhoudt, D. N. *J. Am. Chem. Soc.* **2004**, *126*, 6784−6797.
(29) Zhou, H.-X. *Biophys. J.* **2006**, *91*, 3170−3181.
(30) Wang, S.; Dormidontova, E. E. *Biomacromolecules* **2010**, *11*, 1785−1795.
(31) Sheth, S.; Leckband, D. E. *Proc. Natl. Acad. Sci. U.S.A.* **1997**, *94*, 8399−8404.
(32) Israelachvili, J. *Proc. Natl. Acad. Sci. U.S.A.* **1997**, *94*, 8378−8379.
(33) Vivarès, D.; Belloni, L.; Tardieu, A.; Bonneté, F. *Eur. Phys. J. E* **2002**, *9*, 15−25.
(34) Sheth, S.; Efremova, N.; Leckband, D. E. *J. Phys. Chem. B* **2000**, *104*, 7652−7662.
(35) Leckband, D.; Israelachvili, J. *Q. Rev. Biophys.* **2001**, *34*, 105−267.
(36) Zhou, H.-X.; Rivas, G.; Minton, A. P. *Annu. Rev. Biophys.* **2008**, *37*, 375−397.
(37) Dhakshnamoorthy, B.; Raychaudhury, S.; Blachowicz, L.; Roux, B. *J. Mol. Biol.* **2010**, *396*, 293−300.
(38) Hill, A. V. *J. Physiol.* **1910**, *40*, iv−vii.
(39) Lee, B.; Richards, F. M. *J. Mol. Biol.* **1971**, *55*, 379−400.
(40) Connolly, M. L. *Science* **1983**, *221*, 709−713.
(41) Shrake, A.; Rupley, J. A. *J. Mol. Biol.* **1973**, *79*, 351−364.
(42) Dacheng, W.; Kang, J. *Sci. China, Ser. B* **1996**, *39*, 608−617.
(43) Chandler, D. *Nature* **2005**, *437*, 640−647.
(44) Ashbaugh, H. S.; Kaler, E. W.; Paulaitis, M. E. *J. Am. Chem. Soc.* **1999**, *121*, 9243−9244.
(45) Wagoner, J. A.; Baker, N. A. *Proc. Natl. Acad. Sci. U.S.A.* **2006**, *103*, 8331−8336.
(46) Hermann, R. B. *Proc. Natl. Acad. Sci. U.S.A.* **1977**, *74*, 4144−4145.
(47) Sharp, K. A.; Nicholls, A.; Fine, R. F.; Honig, B. *Science* **1991**, *252*, 106−109.
(48) Berman, H. M.; Westbrook, J.; Feng, Z.; Gilliland, G.; Bhat, T. N.; Weissig, H.; Shindyalov, I. N.; Bourne, P. E. *Nucleic Acids Res.* **2000**, *28*, 235−242.
(49) Yaffe, M. B. *FEBS Lett.* **2002**, *513*, 53−57.
(50) Liu, D.; Bienkowska, J.; Petosa, C.; Collier, R. J.; Fu, H.; Liddington, R. *Nature* **2002**, *376*, 191−194.
(51) Xiao, B.; Smerdon, S. J.; Jones, D. H.; Dodson, G. G.; Soneji, Y.; Aitken, A.; Gamblin, S. J. *Nature* **2002**, *376*, 188−191.
(52) Zhao, J.; Du, Y.; Horton, J. R.; Upadhyay, A. K.; Lou, B.; Bai, Y.; Zhang, X.; Du, L.; Li, M.; Wang, B.; Zhanga, L.; Barbieri, J. T.; Khuri, F. R.; Cheng, X.; Fu, H. *Proc. Natl. Acad. Sci. U.S.A.* **2011**, *108*, 16212−16216.
(53) Yaffe, M. B.; Rittinger, K.; Volinia, S.; Caron, P. R.; Aitken, A.; Leffers, H.; Gamblin, S. J.; Smerdon, S. J.; Cantley, L. C. *Cell* **1997**, *91*, 961−971.
(54) Mack, E. T.; Snyder, P. W.; Perez-Castillejos, R.; Bilgiçer, B.; Moustakas, D. T.; Butte, M. J.; Whitesides, G. M. *J. Am. Chem. Soc.* **2012**, *134*, 333−345.
(55) LaFratea, A. L.; Carlsona, K. E.; Katzenellenbogen, J. A. *Bioorg. Med. Chem.* **2009**, *17*, 3528−3535.
(56) Abendroth, F.; Bujotzek, A.; Shan, M.; Haag, R.; Weber, M.; Seitz, O. *Angew. Chem., Int. Ed.* **2011**, *50*, 8592−8596.
(57) Shiau, A. K.; Barstad, D.; Loria, P. M.; Cheng, L.; Kushner, P. J.; Agard, D. A.; Greene, G. L. *Cell* **1998**, *95*, 927−937.